energy&fuels

Article

pubs.acs.org/EF

Importance of the Hydrogen Isocyanide Isomer in Modeling Hydrogen Cyanide Oxidation in Combustion

Peter Glarborg*[,†] and Paul Marshall[‡]

[†]DTU Chemical Engineering, Technical University of Denmark, 2800 Lyngby, Denmark

[‡]Department of Chemistry and Center for Advanced Scientific Computing and Modeling (CASCaM), University of North Texas, 1155 Union Circle #305070, Denton, Texas 76203-5017, United States

Supporting Information

ABSTRACT: Hydrogen isocyanide (HNC) has been proposed as an important intermediate in oxidation of hydrogen cyanide (HCN) in combustion, but details of its chemistry are still in discussion. At higher temperatures, HCN and HNC equilibrate rapidly, and being more reactive than HCN, HNC offers a fast alternative route of oxidation for cyanides. However, in previous modeling, it has been required to omit the HNC subset partly or fully in the reaction mechanisms to obtain satisfactory predictions. In the present work, we re-examine the chemistry of HNC and its role in combustion nitrogen chemistry. The HNC + O_2 reaction is studied by *ab initio* methods and is shown to have a high barrier. Consequently, the omission of this reaction in recent modeling studies is justified. With the present knowledge of the HNC chemistry, including an accurate value of the heat of formation for HNC and improved rate constants for HNC + O_2 and HNC + OH, it is possible to reconcile the modeling issues and provide a satisfactory prediction of a wide range of experimental results on HCN oxidation. In the burned gases of fuel-rich flames, HCN and the CN radical are partially equilibrated and the sequence HCN $\xrightarrow{+M}$ HNC $\xrightarrow{+OH}$ HNCO is the major consumption path for HCN. Under lean conditions, HNC is shown to be less important than indicated by the early work by Lin and co-workers, but it acts to accelerate HCN oxidation and promotes the formation of HNCO.

INTRODUCTION

In combustion processes, cyanides may be formed from devolatilization of fuels with organically bound nitrogen, from reaction of hydrocarbon radicals (CH and C) with N_2 (the initiating step in prompt NO formation), from reaction of reactive nitrogen species, such as NO or amines, with hydrocarbon radicals, or from decomposition of hydrocarbon amines.[1−5] In sufficiently fuel-rich hydrocarbon flames, it appears that hydrogen cyanide (HCN) is the dominant nitrogenous species leaving the primary reaction zone, regardless of the source of nitrogen,[6−8] and it is considered the predominant cyanide species in combustion. The oxidation chemistry of HCN has been studied extensively over the years. Much of this work was reviewed recently by Dagaut et al.[9]

An unresolved issue in the oxidation chemistry of HCN is the role of its isomer, hydrogen isocyanide (HNC). As suggested initially by Lin et al.,[10] isomerization of HCN to HNC, followed by oxidation of HNC, represents an alternative pathway for HCN oxidation. The reactivity of HNC is quite different from that of HCN, and the presence of HNC in significant quantities may affect the oxidation behavior of HCN. HNC is formed by isomerization of HCN

$$\mathrm{HCN + M \rightleftharpoons HNC + M} \quad \text{(R2)}$$

or by a H atom exchange reaction of HCN with H.

$$\mathrm{HCN + H \rightleftharpoons HNC + H} \quad \text{(R12b)}$$

At high temperatures, these reactions lead to fast equilibration of HNC with HCN. Once formed, HNC has been proposed to react rapidly with OH and O_2.[11]

$$\mathrm{HNC + OH \rightleftharpoons HNCO + H} \quad \text{(R14)}$$

$$\mathrm{HNC + O_2 \rightleftharpoons HNCO + O} \quad \text{(R16a)}$$

$$\mathrm{HNC + O_2 \rightleftharpoons NH + CO_2} \quad \text{(R16b)}$$

Because these steps are presumably much faster than the corresponding reactions of HCN with OH and O_2, they serve to enhance the consumption rate of HCN and convert the cyanide pool to isocyanide species and amines. According to Dagaut et al.,[9] the impact of HNC on HCN consumption is most pronounced for the conditions in shock tubes and flow reactor systems, while it is less important in laminar premixed flames. However, inclusion of a kinetic subset for HNC with the accepted thermochemistry for this species and rate constants for HNC reactions drawn from the evaluation of Dean and Bozzelli[11] leads to a considerable reduction in the accuracy of modeling predictions when compared to experimental data.[9] To obtain acceptable modeling accuracy, Dagaut et al.[9] omitted HNC + O_2 (reaction R16) from their reaction mechanism; otherwise, predicted ignition delays for HCN under shock-tube conditions were too low by an order of magnitude. Dagaut et al. concluded in their review that further work was needed to assess the kinetics of HNC reactions, in particular that of HNC + O_2. This suggestion was supported by

Special Issue: In Honor of Professor Brian Haynes on the Occasion of His 65th Birthday

Received: August 18, 2016
Revised: October 5, 2016
Published: October 5, 2016

DOI: 10.1021/acs.energyfuels.6b02085
Energy Fuels 2017, 31, 2156−2163

Table 1. Values Reported in the Literature for the Thermodynamic Properties of HNC (Heat of Formation of HNC and the Energy Difference between HNC and HCN)

$\Delta H^\circ_{f,298}$(HNC) − $\Delta H^\circ_{f,298}$(HCN) (kcal mol^{-1})	$\Delta H^\circ_{f,298}$(HNC) (kcal mol^{-1})	method	reference
14.6	45.5[a]	theory	15
15.0 ± 2	45.9 ± 2[a]	theory	20
10.3 ± 1.1	41.2 ± 1.1[a]	experimental	22
>17	>47.9[a]	experimental	23
14.8 ± 2	45.7 ± 2[a]	experimental	24
14.4 ± 1	45.3 ± 1[a]	theory	32
12.9	43.8[a]	theory	10
14.7	45.6	theory	34
15.2	46.1[a]	theory	35
15.2	46.1[a]	theory	38
13.8	44.7[a]	theory	76
14.4	45.3 ± 1[a]	experimental	42
14.0 ± 1[b]	44.9 ± 1	experimental	77
18.8 ± 2.9[b]	49.7 ± 2.9	experimental	45
14.7 ± 0.14	45.6 ± 0.14[a]	theory	46
14.2	45.1[a]	theory	52
16.3	47.2[a]	experimental and theory	61
14.2	45.1[a]	theory	62
15.07	45.95 ± 0.09	theory and ATcT	67

[a]Estimated from $\Delta H^\circ_{f,298}$(HNC) − $\Delta H^\circ_{f,298}$(HCN), assuming $\Delta H^\circ_{f,298}$(HCN) = 30.9 kcal mol^{-1}.[67] [b]Estimated from $\Delta H^\circ_{f,298}$(HNC), assuming $\Delta H^\circ_{f,298}$(HCN) = 30.9 kcal mol^{-1}.[67]

Table 2. Thermodynamic Properties of Selected Species in the Reaction Mechanism[a]

species	H_{298}	S_{298}	$C_{p,300}$	$C_{p,400}$	$C_{p,500}$	$C_{p,600}$	$C_{p,800}$	$C_{p,1000}$	$C_{p,1500}$
HCN	31.02	48.23	8.59	9.36	9.97	10.48	11.31	12.01	13.20
HNC	45.95	49.11	9.64	10.22	10.61	10.92	11.55	12.08	13.09
CN	105.15	48.42	6.97	7.04	7.16	7.32	7.69	7.99	8.48

[a]Units are kcal mol^{-1} for H and cal mol^{-1} K^{-1} for S and C_p. Temperatures are in kelvin. Data are drawn from the thermodynamic database of Goos et al.,[78] except that the heat of formation of HNC was updated according to the work of Nguyen et al.[67]

Gimenez-Lopez et al.[12] in a recent flow reactor study on HCN oxidation in a CO_2/N_2 atmosphere, where they found inclusion of the HNC + O_2 reaction to lead to overprediction of the HCN consumption rate.

While the importance of HNC in combustion systems has attracted only modest interest,[9−11,13,14] the properties of HNC have been studied extensively[15−67] in part as a result of its small size, which allows for study at high levels of theory, and in part as a result of its potential importance in astrochemistry. The objective of the present work is to re-evaluate the HNC chemistry, with particular emphasis on HNC + O_2, which is studied by *ab initio* methods, and assess the implications for modeling HCN oxidation in combustion.

DETAILED KINETIC MODEL AND *AB INITIO* CALCULATIONS

The cyanide subset of the chemical kinetic model was based on the work of Dagaut et al.[9] In the present study, the thermochemistry of HNC and rate constants for the reactions involved in forming or consuming HNC were re-evaluated. In addition, the hydrogen and amine chemistry subsets were updated on the basis of recent work.[5,68−75] The full model is available as Supporting Information.

The thermodynamic properties of HNC are important, because they determine the HNC/HCN ratio at high temperatures where the two isomers equilibrate rapidly. Table 1 summarizes the values reported in the literature for the heat of formation of HNC and the energy difference between HNC and HCN. The early experimental determinations of the energy separation between the isomers range from 10.3[22] to more than 17 kcal mol^{-1},[23] but more recent work serves to reduce the uncertainty. Most theoretical predictions[15,20,32,34,35,38,42,46,52,62,67] support a value for $\Delta H^\circ_{f,298}$(HNC) − $\Delta H^\circ_{f,298}$(HCN) of 14.2−15.3 kcal mol^{-1}, in agreement with the experimental value of 14.8 kcal mol^{-1} from Pau and Hehre.[24]

The Pau and Hehre results were questioned by Wenthold[45] based on revisions in the proton affinity scale in later years. From experimental work as well as a reinterpretation of the results of Pau and Hehre, Wenthold obtained a value for the heat of formation of HNC of $\Delta H^\circ_{f,298}$(HNC) = 49.7 ± 2.9 kcal mol^{-1}, corresponding to an energy difference between HNC and HCN of 18.8 ± 2.9 kcal mol^{-1}. A high value was also obtained recently by Barber et al.[61] from a high-level multireference configuration interaction study. They found an energy difference between HNC and HCN of 16.3 kcal mol^{-1}, corresponding to a heat of formation for HNC of 47.2 kcal mol^{-1}.

The high values of $\Delta H^\circ_{f,298}$(HNC) determined by Wenthold[45] and Barber et al.[61] would diminish the importance of HNC in combustion modeling. However, they are called into question in the recent study by Nguyen et al.,[67] who investigated the HCN → HNC 0 K isomerization energy by combining state-of-the-art electronic structure methods with the active thermochemical tables (ATcT) approach. They found the energy difference between HCN and HNC at 298 K to be 15.1 kcal mol^{-1}. This is substantially lower than the values of Barber et al. and Wenthold (by 1.2 and 3.7 kcal mol^{-1}, respectively). Nguyen et al. concluded that the value from Barber et al. was likely to have a much larger uncertainty than originally stated. The analysis from Nguyen et al. indicates that the heat of formation of HNC at 298 K is 45.95 ± 0.09 kcal mol^{-1}; we have adopted this value in the present work. An energy separation between HNC and HCN of 15.1 kcal mol^{-1} is 2.2 kcal mol^{-1} higher than that used in the early study by Lin et al.[10] and adopted by Dean and Bozzelli[11] and recently by

DOI: 10.1021/acs.energyfuels.6b02085
Energy Fuels 2017, 31, 2156−2163

Table 3. Selected Reactions in the HCN Subset[a]

		A	β	E_a	source
1	HCN + M ⇌ CN + H + M[b]	3.4×10^{35}	−5.130	133000	81
	HCN + N_2 ⇌ CN + H + N_2	3.6×10^{26}	−2.600	124890	
2	HCN + M ⇌ HNC + M[c]	1.6×10^{26}	−3.230	51840	11[d]
3	CN + H_2 ⇌ HCN + H	1.1×10^{5}	2.600	51908	82
4	HCN + O ⇌ NCO + H	1.4×10^{4}	2.640	4980	1
5	HCN + O ⇌ NH + CO	3.5×10^{3}	2.640	4980	1
6	HCN + O ⇌ CN + OH	4.2×10^{10}	0.400	20665	11
7	HCN + OH ⇌ CN + H_2O	3.9×10^{6}	1.830	10300	83
8	HCN + OH ⇌ HOCN + H	5.9×10^{4}	2.430	12500	84
9	HCN + OH ⇌ HNCO + H	2.0×10^{-3}	4.000	1000	84
10	HCN + OH ⇌ NH_2 + CO	7.8×10^{-4}	4.000	4000	84
11	HCN + O_2 ⇌ CN + HO_2	3.0×10^{13}	0.000	75100	9 est
12	HNC + H ⇌ HCN + H	7.8×10^{13}	0.000	3600	85
13	HNC + O ⇌ NH + CO	4.6×10^{12}	0.000	2200	11
14	HNC + OH ⇌ HNCO + H	3.6×10^{12}	0.000	−479	86[e]
15	HNC + OH ⇌ CN + H_2O	3.0×10^{2}	3.160	10600	pw
16	HNC + O_2 → products		slow		pw[f]

[a]Parameters for use in the modified Arrhenius expression $k = AT^{\beta} \exp(-E_a/[RT])$. Units are mol, cm, s, and cal. [b]Third body efficiencies: N_2 = 0, O_2 = 1.5, and H_2O = 10. [c]Third body efficiencies: Ar = 0.7, H_2O = 7, and CO_2 = 2. [d]The activation energy was modified according to the updated heat of formation of HNC. [e]Arrhenius expression fitted from data in the reference. [f]The HNC + O_2 reaction has a calculated barrier of 44 kcal mol^{-1} and was not included in the modeling.

Lamoureux et al.,[14] and 0.3 kcal mol^{-1} higher than the recommendation of Dagaut et al.[9]

Table 2 lists thermodynamic properties for HNC, HCN, and cyanide (CN). The thermodynamic properties in the present work were generally adopted from the ideal gas thermochemical database by Goos et al.,[78] with properties obtained using the ATcT approach.[79,80]

Table 3 lists key reactions of HCN and HNC from the chemical kinetic model. There are no reported experimental studies of HNC reactions, and rate constants have been obtained from theory. However, from the available theoretical studies, it is obvious that the reactivity of HNC is quite different from that of HCN. HNC can be formed by isomerization of HCN

$$\mathrm{HCN + M \rightleftharpoons HNC + M} \qquad \text{(R2)}$$

or by reaction of HCN with H.

$$\mathrm{HCN + H \rightleftharpoons HNC + H} \qquad \text{(R12b)}$$

The isomerization step has been studied extensively by theory.[10,11,32,34,35,38,42,49,52,53,64] Estimates of the barrier for the isomerization range from 44.7 to 48.2 kcal mol^{-1}.[10,11,32,34,35,38,42] With a barrier of this magnitude, isomerization (reaction R2) is much faster than thermal dissociation of HCN (reaction R1) and HCN will isomerize fairly easily to HNC at medium to high temperatures. Following Dagaut et al.,[9] we have adopted the rate constant for reaction R2 from the evaluation of Dean and Bozzelli[11] but modified the activation energy to reflect the larger energy separation between HCN and HNC. Also, reaction R12b has been studied theoretically;[85,87] we have included this step in the exothermic direction, HNC + H ⇌ HCN + H (R12), with a rate constant calculated by Sumathi and Nguyen.[85]

The most important consumption reaction of HNC is presumably HNC + OH.

$$\mathrm{HNC + OH \rightleftharpoons HNCO + H} \qquad \text{(R14)}$$

Figure 1 shows an Arrhenius plot for the reaction. In their early evaluation, Lin et al.[10] calculated an activation energy for reaction R14 of 3.7 kcal mol^{-1}. Recently, the reaction was studied at a high level of theory by Bunkan et al.[86] for the 250–350 K range. They predict the rate constant to have a slight negative temperature dependence, at least at low temperatures.

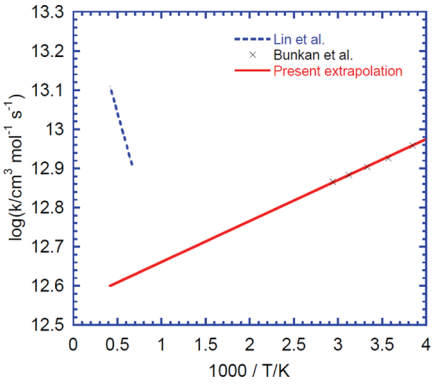

Figure 1. Arrhenius plot for the reaction HNC + OH ⇌ HNCO + H. The symbols denote high level theory data from Bunkan et al.,[86] while the dashed line denotes the rate constant calculated by Lin et al.[10] The solid line is our extrapolation of the data of Bunkan et al. to relevant temperatures.

Their reaction path shows a pre-reaction complex followed by a transition state (TS), whose energy is ∼1.1 kcal mol^{-1} below that of the reactants. Their Rice–Ramsperger–Kassel–Marcus (RRKM) kinetic analysis should correctly allow for the lack of population of energy levels of the TS below the reactants at modest pressures. On the basis of a recomputation of the unpublished CCSD(T) frequencies of the TS, we have made a preliminary assessment of the high pressure limit via transition state theory. This calculation indicates that $k_{14,\infty}$ may reach a minimum and then increase at higher temperatures. However, more work is required to calculate accurately the effect of the temperature and pressure on this reaction. In the current work, we have extrapolated directly the results from Bunkan et al. to higher temperatures with a small negative activation energy (Figure 1) fitted to the published k_{14} values.

For the possible other product channel

$$\mathrm{HNC + OH \rightleftharpoons CN + H_2O} \qquad \text{(R15)}$$

Bunkan et al. deduced a barrier of more than 16 kcal mol^{-1}, which makes that channel too slow to compete under atmospheric

DOI: 10.1021/acs.energyfuels.6b02085
Energy Fuels 2017, 31, 2156–2163

conditions. A combination of their barrier with M06-2X/6-311+G-(3df,2p) vibrational frequencies and geometry for the TS leads to a predicted rate constant of $3.0 \times 10^2 T^{3.16} \exp(-5330/T)$ cm^3 mol^{-1} s^{-1} over 600−3000 K. Tunneling makes a major contribution; thus, there is considerable uncertainty in this expression, perhaps an order of magnitude at the lower end of the temperature range.

For the reaction of HNC with O

$$\mathrm{HNC + O \rightleftharpoons NH + CO} \quad \text{(R13)}$$

we adopt the rate constant proposed by Lin et al.[10] from a combined experimental and theoretical study. Unfortunately, the experimental results referred to by Lin et al. were never published, and more work on this step is desirable.

Dean and Bozzelli suggested that oxygen could readily add to HNC and that subsequent isomerization or dissociation steps would lead to HNCO + O and NH + CO_2.[11]

$$\mathrm{HNC + O_2 \rightleftharpoons HNCO + O} \quad \text{(R16a)}$$

$$\mathrm{HNC + O_2 \rightleftharpoons NH + CO_2} \quad \text{(R16b)}$$

They computed low barriers for both channels and obtained rate constants of $k_{16a} = 1.5 \times 10^{12} T^{0.01} \exp(-2068/T)$ cm^3 mol^{-1} s^{-1} and $k_{16b} = 1.6 \times 10^{19} T^{-2.25} \exp(-896/T)$ cm^3 mol^{-1} s^{-1}. However, Dagaut et al.[9] found it necessary to omit the HNC + O_2 reactions in their modeling study to obtain consistency with experimental results. More recently, Gimenez-Lopez et al.[12] and Lamoreux et al.[14] also disregarded HNC + O_2 in their reaction mechanisms. This prompted us to characterize the reaction by *ab initio* methods.

We find that a triplet HNCOO adduct lies ca. 42 kcal mol^{-1} above HNC + O_2 at the CBS-QB3 level of theory, and the barrier to forming this adduct (including zero-point energy) is even higher, at about 44 kcal mol^{-1}, which is confirmed by CCSD(T)/cc-pVTZ calculations.[88,89] The high energy barrier makes the reaction insignificant under most conditions of interest. Singlet HNCOO is even less stable.

The reaction of HCN with OH is of particular interest in this work, because it competes directly with HNC + OH (reaction R14). It is a complicated process, involving multiple potential wells and multiple product channels.[1]

$$\mathrm{HCN + OH \rightleftharpoons CN + H_2O} \quad \text{(R7)}$$

$$\mathrm{HCN + OH \rightleftharpoons HOCN + H} \quad \text{(R8)}$$

$$\mathrm{HCN + OH \rightleftharpoons HNCO + H} \quad \text{(R9)}$$

$$\mathrm{HCN + OH \rightleftharpoons NH_2 + CO} \quad \text{(R10)}$$

The rate constant for the H-abstraction channel to form CN + H_2O (reaction R7) has been measured directly in both the forward and reverse directions. Figure 2 shows an Arrhenius plot for this step. Wooldridge et al.[83] determined k_7 from CN and OH time histories in shock-tube experiments. The results shown from Jacobs et al.[90] were obtained for the reverse reaction and have been converted using the present thermodynamic properties for the involved species. The two data sets are in very good agreement, indicating that the rate constant for this reaction is known quite accurately. The experiments of Wooldridge et al. are analyzed further below.

For the other product channels of HCN + OH (reactions R8−R10), rate constants are drawn from BAC-MP4 calculations by Miller and Melius.[84] There are no experimental data for these product channels, and more work is desirable to support the rate constants. At most conditions, the H-abstraction reaction (reaction R7) dominates, but at very low temperatures, the formation of HNCO + H (reaction R9) is competitive, while at temperatures above 2000 K, HOCN + H (reaction R8) becomes the fastest channel.

RESULTS AND DISCUSSION

This section aims to clarify the role of HNC in oxidation of HCN at medium to high temperatures relevant for combustion. HCN is presumably the most important precursor of HNC in

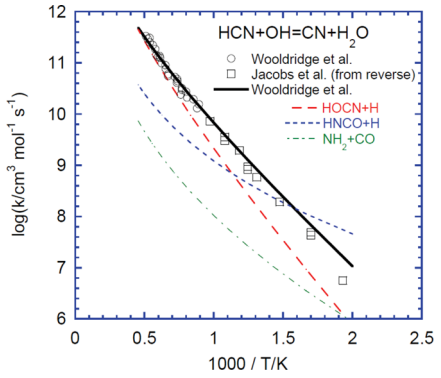

Figure 2. Arrhenius plot for the reaction HCN + OH ⇌ CN + H_2O (R7). The symbols denote experimental results from Wooldridge et al.[83] and from Jacobs et al.[90] (from measurements of CN + H_2O, reversed through the equilibrium constant), while the solid line shows the constant recommended by Wooldridge et al. Also shown (dashed lines) are rate constants for the secondary channels to HOCN + H (reaction R8), HNCO + H (reaction R9), and NH_2 + CO (reaction R10), drawn from BAC-MP4 calculations by Miller and Melius.[84]

combustion, and the expected role of HNC is to accelerate the HCN consumption, converting it to isocyanides and amines.

Haynes[8] investigated the decay of HCN in the burnt gases of a number of fuel-rich, atmospheric pressure hydrocarbon flames. Independent of the type of nitrogen additive (ammonia or pyridine), it was converted to HCN in the reaction zone of the flame, with smaller amounts of NO. In the post-flame zone, HCN was slowly converted to NH_3. Haynes found the decay mechanism for HCN at temperatures below 2300 K to be first-order in OH, and he assumed it to be

$$\mathrm{HCN + OH \rightarrow (HOCN) + H}$$

or a kinetically equivalent process, with the (HOCN) isomer eventually converted to NH_3.

Figure 3 compares measurements by Haynes for a rich ethylene flame doped with ammonia to modeling predictions. The temperature of the burnt gases was 2000 K. In the modeling predictions, only the post-flame zone was considered.

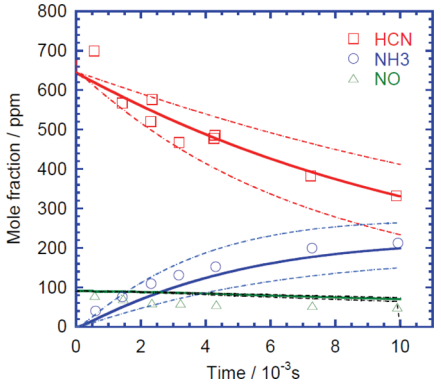

Figure 3. Comparison between experimental data[8] and modeling predictions for HCN oxidation in the post-flame region of an atmospheric pressure, premixed, fuel-rich ethylene−air flame doped with 680 ppm of ammonia. Fuel-air equivalence ratio ϕ = 1.66, and temperature = 2000 K. Symbols denote experimental data, while lines denote model predictions. Solid lines denote predictions with the present model, while dashed lines show the effect of varying the rate constant k_{14} for HNC + OH by a factor of 2.

DOI: 10.1021/acs.energyfuels.6b02085
Energy Fuels 2017, 31, 2156−2163

It was assumed that both acetylene and oxygen were depleted in the reaction zone, resulting in an equilibrium mixture of CO, H_2, CO_2, and H_2O entering the post-flame zone. In the calculations, the equilibrium composition at 2000 K, together with the measured concentrations of HCN, NH_3, and NO, was used as the inlet composition. The modeling predictions (solid lines) are in good agreement with the measurements for HCN, NH_3, and NO. Analysis of the present calculations indicates that HCN is consumed through a two-step sequence.

$$HCN + M \rightleftharpoons HNC + M \quad (R2)$$

$$HNC + OH \rightleftharpoons HNCO + H \quad (R14)$$

This sequence is kinetically equivalent to the reaction proposed by Haynes. Under the conditions in the flame, HCN equilibrates rapidly with HNC. Atomic hydrogen and to a lesser extent OH are the dominant radicals in the flame, but they consume little HCN because the reactions HCN + H ⇌ CN + H_2 (R3b) and HCN + OH ⇌ CN + H_2O (R7) are both rapidly equilibrated. This makes the conditions favorable to study the reactions of HNC, in particular HNC + OH (reaction R14), even though other product channels for HCN + OH, in particular reaction R8, are also active. The HNCO formed in reaction R14 feeds rapidly into the amine pool, eventually forming NH_3.

$$HNCO + H \rightleftharpoons NH_2 + CO$$

$$NH_2 + H_2 \rightleftharpoons NH_3 + H$$

A smaller fraction of NH_2 is converted to NH and N through the sequence $NH_2 \xrightarrow{+H} NH \xrightarrow{+H} N$. The NH and N radicals may be oxidized to NO by reaction with OH or react with NO to form N_2O or N_2. This competition results overall in a small decrease in the NO concentration.

In Figure 3, dashed lines show predictions with the rate constant for HNC + OH (reaction R14) varied by a factor of 2. The results show that the predicted HCN and NH_3 profiles are quite sensitive to the value of k_{14}. This is confirmed by Figure 4,

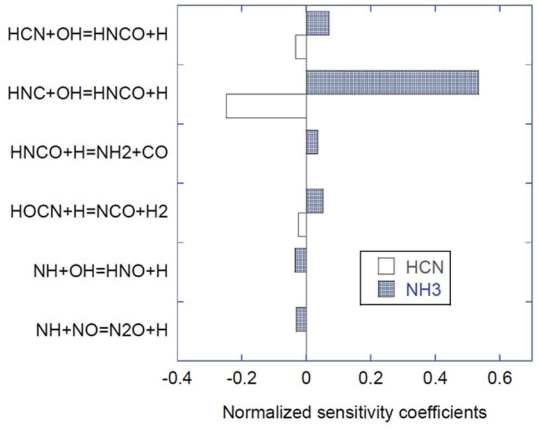

Figure 4. First-order sensitivity coefficients for HCN and NH_3 for the conditions of the flame in Figure 3.

which shows the results of a sensitivity analysis for HCN and NH_3 for the conditions of Figure 3. For HCN, the rate constant for reaction R14 has by far the largest sensitivity coefficient. Also, the predicted NH_3 concentration is sensitive mostly to this step. The good agreement obtained in modeling for both of these species supports the accuracy of k_{14} at this temperature. The OH radical maintains a partial equilibrium in the post-flame region, and modeling predictions are not sensitive to chain-branching or terminating steps.

For high-temperature conditions in a shock tube, the isomerization of HCN to HNC is sufficiently rapid to occur at the same microsecond time scale as the observed chemistry[11] and predicted induction times for HCN/O_2 mixtures are quite sensitive to the HNC subset.[9] Higashihara et al.[91] studied the oxidation of HCN by O_2 in a shock tube over the temperature range of 1450−2600 K and pressures of 0.75−2.0 atm. They measured the ultraviolet (UV) signal from electronically excited OH and defined the induction time τ_{OH^*} as the time where the UV emission started to increase rapidly. OH* was assumed to be formed largely from recombination of O and H radicals. For the HCN/O_2 system, the OH* induction time from a least squares analysis could be represented as $\tau_{OH^*} = 10^{-13.42} \exp(-12200/T)[HCN]^{-0.44}[O_2]^{-0.17}[Ar]^{-0.52}$ s.

In Figure 5, data estimated from this empirical expression are compared to predictions using the chemical kinetic model. In

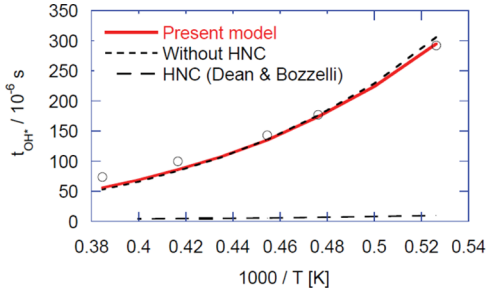

Figure 5. Comparison between measured[91] and predicted induction times as a function of the temperature for oxidation of HCN (1%) by O_2 (1%) in argon in a shock tube. The experimental data are derived from the least squares analysis expression by Higashihara et al., assuming P = 1.0 atm. In the calculations, the induction time is taken as the time to reach 25% of the peak concentration for O. Experimental data are shown as symbols, while modeling predictions are shown as lines.

this figure as well as in the following, modeling predictions are shown for three different mechanisms: (1) full present mechanism, (2) present mechanism excluding the HNC subset, and (3) present mechanism with $\Delta H^\circ_{f,298}(HNC) - \Delta H^\circ_{f,298}(HCN)$ = 12.9 kcal mol^{-1}[10,11,14] and rate constants from Dean and Bozzelli,[11] including the HNC + O_2 reaction.

In the modeling of the data in Figure 5, the OH* induction time is defined as the time to reach 25% of the peak concentration of O. Predictions with the present model with (solid line) and without (short dashed line) the HNC subset are both in good agreement with the measured induction times. The similarity between predictions with and without HNC indicates that this species, with the present chemistry, plays only a small role under these conditions. However, if the HNC subset is replaced by that recommended by Dean and Bozzelli,[11] the predicted induction time is lowered by more than a factor of 10, in conflict with the experimental observations. The too low value for the energy separation between HNC and HCN contributes to the discrepancy, because it leads to overprediction of the HNC concentration. However, most of the difference is caused by the fast rate constants for HNC + O_2 estimated by Dean and Bozzelli.

Wooldridge et al.[83] measured CN and OH time histories in incident and reflected shock waves using dilute mixtures of

DOI: 10.1021/acs.energyfuels.6b02085
Energy Fuels 2017, 31, 2156−2163

HCN and nitric acid (HNO_3) in argon. The thermal decomposition of HNO_3 yielded OH upon shock heating, and OH subsequently reacted predominantly with HCN. As discussed above, they used the data to deduce a rate constant for the reaction HCN + OH ⇌ CN + H_2O (R7). Their simultaneous measurements of CN and OH yielded values of k_7 in good agreement, putting severe limitations on the importance of the HNC isomer. Wooldridge et al. concluded that they had to omit reactions of HNC to obtain a satisfactory agreement between their observed concentration profiles and modeling results. A further constraint on HNC + OH is the excellent consistency between the two data sets from Wooldridge et al. and Jacobs et al.[90] (Figure 2). Apparently, HNC + OH cannot have had a significant impact on the OH concentration profile in the experiments of Wooldridge et al.

Figure 6 shows a comparison between experimental results obtained at 1492 K and modeling predictions to the present

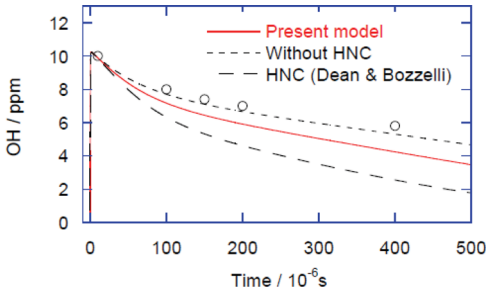

Figure 6. Comparison between measured[83] and predicted OH absorption traces from the reflected shock pyrolysis of 10.3 ppm of HNO_3 and 0.34% HCN in argon for T = 1492 K and P = 1.01 atm. Experimental data are shown as symbols, while modeling predictions are shown as lines.

reaction mechanism. For these conditions, Wooldridge et al. reported only the OH concentration profile; at higher temperatures, where concentrations were reported for both OH and CN, predictions are less sensitive to reactions of HNC because HCN + OH becomes more competitive. As expected, the model (solid line) is seen to overestimate the OH consumption rate. The discrepancy, which is due to OH consumption by HNC + OH (reaction R14), can be removed by taking out HNC from the reaction mechanism (short dashed line), as proposed by Wooldridge et al. However, we find the level of agreement to be satisfactory because it is within the 30% overall uncertainty attributed to k_7 by Wooldridge et al. as a result of uncertainties in side reactions. As expected, predictions with the Dean and Bozzelli HNC subset (long dashed line) show a larger deviation, partly as a result of the difference in thermochemistry and partly as a result of a faster rate constant for HNC + OH.

Figure 7 compares flow reactor results from Glarborg and Miller[13] on lean HCN oxidation to modeling predictions. The experiments were conducted at 900−1400 K and atmospheric pressure with a dilute mixture of HCN, O_2, and H_2O in N_2, and the product composition at the reactor outlet was measured. The calculations show a considerable impact of the choice of HNC subset. The preferred model provides a good agreement with the measured profiles of HCN, HNCO, and NO, while omission of the HNC subset leads to delayed onset of the reaction. The Dean and Bozzelli HNC subset leads to premature ignition and a strong underprediction of HNCO.

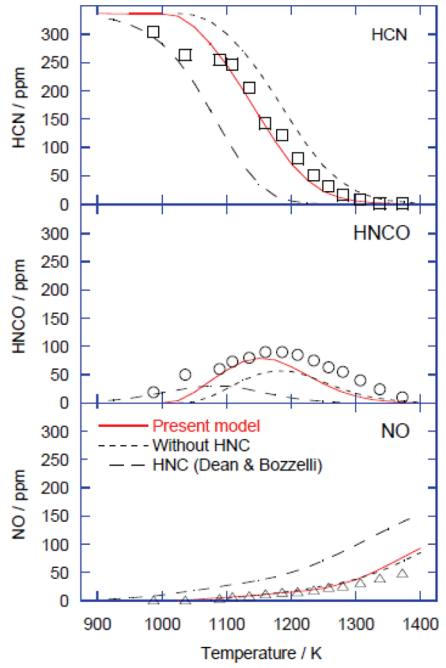

Figure 7. Comparison between experimental data[13] and modeling predictions for HCN oxidation in a flow reactor. Symbols denote experimental data, while lines denote model predictions. Inlet concentrations: 337 ppm of HCN, 2.6% O_2, 3.1% H_2O, and balance N_2. The pressure is 1.05 atm, and the residence time at 1200 K (constant constant mass flow) is 112 ms.

In Figure 8, jet-stirred reactor experiments reported by Dagaut et al.[92] for the oxidation of HCN are compared to

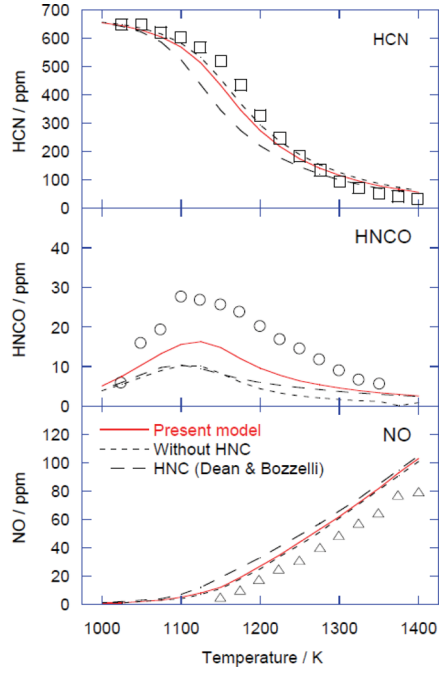

Figure 8. Comparison between experimental data[92] and modeling predictions for HCN oxidation in a jet-stirred reactor. Symbols denote experimental data, while lines denote model predictions. Inlet concentrations: 670 ppm of HCN, 2000 ppm of O_2, 200 ppm of H_2O, and balance N_2. The pressure is 1.0 atm, and the residence time is 120 ms.

DOI: 10.1021/acs.energyfuels.6b02085
Energy Fuels 2017, 31, 2156−2163

modeling predictions. The modeling predictions agree well with the measured profiles for HCN and NO, but HNCO is underpredicted by almost a factor of 2. Exclusion of the HNC subset has only a small impact on HCN and NO predictions but acts to increase the discrepancy for HNCO. Use of the HNC subset from Dean and Bozzelli leads to a too fast calculated consumption of HCN and also has an adverse impact on the HNCO prediction.

CONCLUSION

The chemistry of HNC and its role in combustion nitrogen chemistry have been re-examined. The HNC + O_2 reaction was studied by *ab initio* methods and shown to have a high barrier. With an updated kinetic subset for the HNC chemistry, including an accurate value of the heat of formation for HNC and improved rate constants for HNC + O_2 and HNC + OH, it was possible to reconcile modeling issues and provide a satisfactory prediction of a wide range of experimental results on HCN oxidation. In the burned gases of fuel-rich flames, where HCN and CN are partially equilibrated, the sequence $HCN \xrightarrow{+M} HNC \xrightarrow{+OH} HNCO$ is the major consumption path for HCN. Under lean conditions, HNC is shown to be less important than indicated by the early work of Lin and co-workers but acts to accelerate HCN oxidation and promote the formation of HNCO.

ASSOCIATED CONTENT

Supporting Information

The Supporting Information is available free of charge on the ACS Publications website at DOI: 10.1021/acs.energyfuels.6b02085.

Full model (ASCII) (TXT)

AUTHOR INFORMATION

Corresponding Author

*E-mail: pgl@kt.dtu.dk.

Notes

The authors declare no competing financial interest.

ACKNOWLEDGMENTS

The work is part of the Combustion and Harmful Emission Control (CHEC) research program. It was financially supported by the Technical University of Denmark. Paul Marshall thanks the R. A. Welch Foundation (Grant B-1174) for support. Peter Glarborg thanks Drs. Branko Ruscic, Stephen Klippenstein, and James A. Miller for helpful discussions.

REFERENCES

(1) Miller, J. A.; Bowman, C. T. *Prog. Energy Combust. Sci.* **1989**, *15*, 287−338.
(2) Bowman, C. T. *Symp. Combust., [Proc.]* **1992**, *24*, 859−878.
(3) Glarborg, P.; Jensen, A. D.; Johnsson, J. E. *Prog. Energy Combust. Sci.* **2003**, *29*, 89−113.
(4) Glarborg, P. *Proc. Combust. Inst.* **2007**, *31*, 77−98.
(5) Lucassen, A.; Zhang, K.; Warkentin, J.; Moshammer, K.; Glarborg, P.; Marshall, P.; Kohse-Höinghaus, K. *Combust. Flame* **2012**, *159*, 2254−2279.
(6) Haynes, B. S.; Iverach, D.; Kirov, N. Y. *Symp. Combust., [Proc.]* **1975**, *15*, 1103−1112.
(7) Fenimore, C. P. *Combust. Flame* **1976**, *26*, 249−256.
(8) Haynes, B. S. *Combust. Flame* **1977**, *28*, 113−121.
(9) Dagaut, P.; Glarborg, P.; Alzueta, M. U. *Prog. Energy Combust. Sci.* **2008**, *34*, 1−46.
(10) Lin, M. C.; He, Y.; Melius, C. F. *Int. J. Chem. Kinet.* **1992**, *24*, 1103−1107.
(11) Dean, A. M.; Bozzelli, J. W. Combustion chemistry of nitrogen. In *Gas Phase Combustion Chemistry*; Gardiner, W. C., Ed.; Springer: New York, 2000; Chapter 2, pp 125−341, DOI: 10.1007/978-1-4612-1310-9_2.
(12) Gimenez-Lopez, J.; Millera, A.; Bilbao, R.; Alzueta, M. U. *Combust. Flame* **2010**, *157*, 267−276.
(13) Glarborg, P.; Miller, J. A. *Combust. Flame* **1994**, *99*, 475−483.
(14) Lamoureux, N.; Merhubi, H. E.; Pillier, L.; de Persis, S.; Desgroux, P. *Combust. Flame* **2016**, *163*, 557−575.
(15) Pearson, P. K.; Schaefer, H. F.; Wahlgren, U. *J. Chem. Phys.* **1975**, *62*, 350−354.
(16) Vonniessen, W.; Cederbaum, L. S.; Domcke, W.; Diercksen, G. H. F. *Mol. Phys.* **1976**, *32*, 1057−1061.
(17) Ishida, K.; Morokuma, K.; Komornicki, A. *J. Chem. Phys.* **1977**, *66*, 2153−2156.
(18) Dorschner, R.; Kaufmann, G. *Inorg. Chim. Acta* **1977**, *23*, 97−101.
(19) Gray, S. K.; Miller, W. H.; Yamaguchi, Y.; Schaefer, H. F. *J. Chem. Phys.* **1980**, *73*, 2733−2739.
(20) Redmon, L. T.; Purvis, G. D.; Bartlett, R. J. *J. Chem. Phys.* **1980**, *72*, 986−991.
(21) Vazquez, G. J.; Gouyet, J. F. *Chem. Phys. Lett.* **1981**, *77*, 233−238.
(22) Maki, A. G.; Sams, R. L. *J. Chem. Phys.* **1981**, *75*, 4178−4182.
(23) Maricq, M. M.; Smith, M. A.; Simpson, C. J. S. M.; Ellison, G. B. *J. Chem. Phys.* **1981**, *74*, 6154−6170.
(24) Pau, C. F.; Hehre, W. J. *J. Phys. Chem.* **1982**, *86*, 321−322.
(25) Peric, M.; Mladenovic, M.; Peyerimhoff, S. D.; Buenker, R. J. *Chem. Phys.* **1983**, *82*, 317−336.
(26) Glidewell, C.; Thomson, C. *J. Comput. Chem.* **1984**, *5*, 1−10.
(27) Peric, M.; Mladenovic, M.; Peyerimhoff, S. D.; Buenker, R. J. *Chem. Phys.* **1984**, *86*, 85−103.
(28) Waite, B. A. *J. Phys. Chem.* **1984**, *88*, 5076−5083.
(29) Bacic, Z.; Gerber, R. B.; Ratner, M. A. *J. Phys. Chem.* **1986**, *90*, 3606−3612.
(30) Smith, R. S.; Shirts, R. B.; Patterson, C. W. *J. Chem. Phys.* **1987**, *86*, 4452−4460.
(31) Szalay, V. *J. Chem. Phys.* **1990**, *92*, 3633−3644.
(32) Lee, T. J.; Rendell, A. P. *Chem. Phys. Lett.* **1991**, *177*, 491−497.
(33) Lan, B. L.; Bowman, J. M. *J. Phys. Chem.* **1993**, *97*, 12535−12540.
(34) Bowman, J. M.; Gazdy, B.; Bentley, J. A.; Lee, T. J.; Dateo, C. E. *J. Chem. Phys.* **1993**, *99*, 308−323.
(35) Gazdy, B.; Musaev, D. G.; Bowman, J. M.; Morokuma, K. *Chem. Phys. Lett.* **1995**, *237*, 27−32.
(36) Zhao, M. S. *Chin. J. Chem.* **1995**, *13*, 141−149.
(37) Talbi, D.; Ellinger, Y.; Herbst, E. *Astron. Astrophys.* **1996**, *314*, 688−692.
(38) Talbi, D.; Ellinger, Y. *Chem. Phys. Lett.* **1996**, *263*, 385−392.
(39) Rao, V. S.; Vijay, A.; Chandra, A. K. *Can. J. Chem.* **1996**, *74*, 1072−1077.
(40) Jursic, B. S. *J. Chem. Soc., Faraday Trans.* **1997**, *93*, 2355−2359.
(41) Bowman, J. M.; Gazdy, B. *J. Phys. Chem. A* **1997**, *101*, 6384−6388.
(42) Contreras, R.; Safont, V. S.; Pérez, P.; Andrés, J.; Moliner, V.; Tapia, O. *J. Mol. Struct.: THEOCHEM* **1998**, *426*, 277−288.
(43) Kumeda, Y.; Minami, Y.; Takano, K.; Taketsugu, T.; Hirano, T. *J. Mol. Struct.: THEOCHEM* **1999**, *458*, 285−291.
(44) Christoffel, K. M.; Bowman, J. M. *J. Chem. Phys.* **2000**, *112*, 4496−4505.
(45) Wenthold, P. G. *J. Phys. Chem. A* **2000**, *104*, 5612−5616.
(46) van Mourik, T.; Harris, G. J.; Polyansky, O. L.; Tennyson, J.; Csaszar, A. G.; Knowles, P. J. *J. Chem. Phys.* **2001**, *115*, 3706−3718.
(47) Barber, R. J.; Harris, G. J.; Tennyson, J. *J. Chem. Phys.* **2002**, *117*, 11239−11243.

DOI: 10.1021/acs.energyfuels.6b02085
Energy Fuels 2017, 31, 2156−2163

(48) Liao, X. L.; Wu, W.; Mo, Y. R.; Zhang, Q. N. *Sci. China, Ser. B: Chem.* **2003**, *46*, 361−370.
(49) Isaacson, A. D. *J. Phys. Chem. A* **2006**, *110*, 379−388.
(50) Harris, G. J.; Tennyson, J.; Kaminsky, B. M.; Pavlenko, Y. V.; Jones, H. R. A. *Mon. Not. R. Astron. Soc.* **2006**, *367*, 400−406.
(51) Mellau, G. C.; Winnewisser, B. P.; Winnewisser, M. *J. Mol. Spectrosc.* **2008**, *249*, 23−42.
(52) DePrince, A. E., III; Mazziotti, D. A. *J. Phys. Chem. B* **2008**, *112*, 16158−16162.
(53) Quapp, W.; Zech, A. *J. Comput. Chem.* **2010**, *31*, 573−585.
(54) Mellau, G. C. *J. Chem. Phys.* **2010**, *133*, 164303.
(55) Mellau, G. C. *J. Mol. Spectrosc.* **2010**, *264*, 2−9.
(56) Mellau, G. C. *J. Chem. Phys.* **2011**, *134*, 234303.
(57) Mellau, G. C. *J. Mol. Spectrosc.* **2011**, *269*, 77−85.
(58) Mellau, G. C. *J. Chem. Phys.* **2011**, *134*, 194302.
(59) Mellau, G. C. *J. Mol. Spectrosc.* **2011**, *269*, 12−20.
(60) Hebrard, E.; Dobrijevic, M.; Loison, J. C.; Bergeat, A.; Hickson, K. M. *Astron. Astrophys.* **2012**, *541*, A21.
(61) Barber, R. J.; Strange, J. K.; Hill, C.; Polyansky, O. L.; Mellau, G. C.; Yurchenko, S. N.; Tennyson, J. *Mon. Not. R. Astron. Soc.* **2014**, *437*, 1828−1835.
(62) Vichietti, R. M.; Haiduke, R. L. A. *Mon. Not. R. Astron. Soc.* **2014**, *437*, 2351−2360.
(63) Loison, J. C.; Wakelam, V.; Hickson, K. M. *Mon. Not. R. Astron. Soc.* **2014**, *443*, 398−410.
(64) Gutiérrez-Oliva, J. S.; Díaz, S.; Toro-Labbé, A.; Lane, P.; Murray, J. S.; Politzer, P. *Mol. Phys.* **2014**, *112*, 349−354.
(65) Gutiérrez-Oliva, S.; Díaz, S.; Toro-Labbé, A.; Lane, P.; Murray, J. S.; Politzer, P. *Mol. Phys.* **2014**, *112*, 349−354.
(66) Baraban, J. H.; Changala, P. B.; Mellau, G. C.; Stanton, J. F.; Merer, A. J.; Field, R. W. *Science* **2015**, *350*, 1338−1342.
(67) Nguyen, T. L.; Baraban, J. H.; Ruscic, B.; Stanton, J. F. *J. Phys. Chem. A* **2015**, *119*, 10929−10934.
(68) Hashemi, H.; Christensen, J. M.; Gersen, S.; Glarborg, P. *Proc. Combust. Inst.* **2015**, *35*, 553−560.
(69) Rasmussen, C. L.; Rasmussen, A. E.; Glarborg, P. *Combust. Flame* **2008**, *154*, 529−545.
(70) Tian, Z.; Li, Y.; Zhang, L.; Glarborg, P.; Qi, F. *Combust. Flame* **2009**, *156*, 1413−1426.
(71) Mendiara, T.; Glarborg, P. *Combust. Flame* **2009**, *156*, 1937−1949.
(72) Mendiara, T.; Glarborg, P. *Energy Fuels* **2009**, *23*, 3565−3572.
(73) Klippenstein, S. J.; Harding, L. B.; Glarborg, P.; Miller, J. A. *Combust. Flame* **2011**, *158*, 774−789.
(74) Abian, M.; Alzueta, M. U.; Glarborg, P. *Int. J. Chem. Kinet.* **2015**, *47*, 518−532.
(75) Song, Y.; Hashemi, H.; Christensen, J. M.; Zou, C.; Marshall, P.; Glarborg, P. *Fuel* **2016**, *181*, 358−365.
(76) Talbi, D.; Ellinger, Y. *Chem. Phys. Lett.* **1998**, *288*, 155−164.
(77) Hansel, A.; Scheiring, C.; Glantschnig, M.; Lindinger, W.; Ferguson, E. E. *J. Chem. Phys.* **1998**, *109*, 1748−1750.
(78) Goos, E.; Burcat, A.; Ruscic, B. *Ideal Gas Thermochemical Database with Updates from Active Thermochemical Tables*; ftp://ftp.technion.ac.il/pub/supported/aetdd/thermodynamics mirrored at http://garfield.chem.elte.hu/burcat/burcat.html.
(79) Ruscic, B.; Pinzon, R. E.; Morton, M. L.; von Laszevski, G.; Bittner, S.; Nijsure, S. G.; Amin, K. A.; Minkoff, M.; Wagner, A. F. *J. Phys. Chem. A* **2004**, *108*, 9979−9997.
(80) Ruscic, B.; Pinzon, R. E.; von Laszewski, G.; Kodeboyina, D.; Burcat, A.; Leahy, D.; Montoy, D.; Wagner, A. F. *J. Phys.: Conf. Ser.* **2005**, *16*, 561−570.
(81) Tsang, W.; Herron, J. T. *J. Phys. Chem. Ref. Data* **1991**, *20*, 609−663.
(82) Baulch, D. L.; Bowman, C. T.; Cobos, C. J.; Cox, R. A.; Just, T.; Kerr, J. A.; Pilling, M. J.; Stocker, D.; Troe, J.; Tsang, W.; Walker, R. W.; Warnatz, J. *J. Phys. Chem. Ref. Data* **2005**, *34*, 757−1397.
(83) Wooldridge, S. T.; Hanson, R. K.; Bowman, C. T. *Int. J. Chem. Kinet.* **1995**, *27*, 1075−1087.
(84) Miller, J. A.; Melius, C. F. *Symp. Combust., [Proc.]* **1988**, *21*, 919−927.
(85) Sumathi, R.; Nguyen, M. T. *J. Phys. Chem. A* **1998**, *102*, 8013−8020.
(86) Bunkan, A. J. C.; Tang, Y.; Sellevag, S. R.; Nielsen, C. J. *J. Phys. Chem. A* **2014**, *118*, 5279−5288.
(87) Jiang, B.; Guo, H. *J. Chem. Phys.* **2013**, *139*, 224310.
(88) Montgomery, J. A.; Frisch, M. J.; Ochterski, J. W.; Petersson, G. A. *J. Chem. Phys.* **1999**, *110*, 2822−2827.
(89) Frisch, M. J.; et al. *Gaussian 09*; Gaussian, Inc.: Wallingford, CT, 2000.
(90) Jacobs, A.; Wahl, M.; Weller, R.; Wolfrum, J. *Chem. Phys. Lett.* **1988**, *144*, 203−207.
(91) Higashihara, T.; Saito, K.; Murakami, I. *J. Phys. Chem.* **1983**, *87*, 3707−3712.
(92) Dagaut, P.; Lecomte, F.; Chevailler, S.; Cathonnet, M. *Combust. Sci. Technol.* **2000**, *155*, 105−127.

DOI: 10.1021/acs.energyfuels.6b02085
Energy Fuels 2017, 31, 2156−2163